First-principles approach to the electronic structure in the pentacene thin film polymorph

2007 J. Phys.: Condens. Matter 19 106209

(http://iopscience.iop.org/0953-8984/19/10/106209)

IOP PUBLISHING JOURNAL OF PHYSICS: CONDENSED MATTER

J. Phys.: Condens. Matter **19** (2007) 106209 (10pp) doi:10.1088/0953-8984/19/10/106209

First-principles approach to the electronic structure in the pentacene thin film polymorph

P Parisse[1,4], L Ottaviano[1], B Delley[2] and S Picozzi[3]

[1] Dipartimento di Fisica, Universitá di L'Aquila, Via Vetoio, 10 67010 Coppito, L'Aquila, Italy
[2] Paul Scherrer Institut, WHGA/123, Villigen PSI, Switzerland
[3] Consiglio Nazionale delle Ricerche, Istituto Nazionale di Fisica della Materia (CNR-INFM), CASTI Regional Lab, 67010 Coppito, L'Aquila, Italy

E-mail: pietro.parisse@aquila.infn.it

Received 19 October 2006, in final form 19 January 2007
Published 16 February 2007
Online at stacks.iop.org/JPhysCM/19/106209

Abstract

Density functional theory (DFT) calculations have been performed to investigate the electronic structure of pentacene in the so-called 'thin film' phase, focusing on the effects on the relevant electronic properties of the relative orientation of the molecules within the crystalline unit cell, which are so far experimentally unknown. Our results show that the energy bandwidth and bandgap are crucially affected by the molecular stacking. Furthermore, by comparing our theoretical spectra with scanning tunnelling spectroscopy measurements, we propose a molecular arrangement that gives good agreement with experiments as far as the relevant orbitals are concerned. For this polymorph, we find highest occupied molecular orbital (HOMO) and lowest unoccupied molecular orbital (LUMO) bandwidths of ∼0.7 and ∼0.8 eV, respectively, which are significatively larger than those obtained for the pentacene bulk phase and are consistent with the larger conductivity observed experimentally in pentacene thin films.

(Some figures in this article are in colour only in the electronic version)

1. Introduction

A deep investigation and a thorough understanding of the structural, electronic and transport properties of organic molecules are of great interest for potential applications in nano- and micro-electronics research [1]. A wide variety of molecules have been studied in recent years. Among these, the family of polyacenes is certainly one of the most investigated, as a prototype class. n-acenes are constituted of linear chains of n planar benzenic rings. The structural stability [2], the capability of forming highly ordered polycrystalline films [3, 4], along with the high mobility [5], make pentacene ($C_{22}H_{14}$, $n = 5$) the most promising polyacene for

[4] Author to whom any correspondence should be addressed.

Table 1. Lattice parameters of the bulk phase, as reported by Campbell [11], and of the thin film phase, used in the present work. For the thin film configuration we exchange a with b to compare better our results with the bulk phase.

Crystallographic phase	a (Å)	b (Å)	c (Å)	α (deg)	β (deg)	γ (deg)
Thin film [25]	7.6	5.9	15.43	90	90	90
Bulk [11]	7.90	6.06	16.01	101.9	112.6	85.8

several applications (organic thin film transistors, organic light-emitting diodes, Schottky diodes, and solar cells [6–10]). This organic molecule crystallizes in a triclinic structure with two inequivalent molecules in a herringbone arrangement in the unit cell [11]. However, the growth parameters strongly affect the structural properties, giving rise to polymorphism. In particular, pentacene appears in four distinct phases, which principally differ from each other in the tilting of the molecules with respect to the substrates and in the (001) interplanar distance [12, 13]. In turn, the different molecular stacking in different polymorphs can change the electronic and transport properties remarkably. A series of theoretical and computational works [14–20] has been performed for two polymorphs, namely the 'single crystal' and the 'bulk' phase, for which the structural parameters and molecule positions have been measured experimentally [2, 11, 21, 22]. Modelling and band structure calculations for other polymorphs have been proposed in recent years [12, 13, 23, 24]. However, recent experimental data [25–27] indicate a sligthly different stacking of molecules, resulting in the so-called 'thin film' polymorph. This phase, of interest for organic thin film transistor applications, is observed in polycrystalline thin films (thickness $\leqslant$50 nm) deposited on inert substrates [6, 4, 25, 28] with micrometer-sized grains. Despite its obvious technological relevance, the electronic and transport properties of such a phase are not yet well understood. Therefore, in the present work we focus on this specific polymorph, performing DFT-based calculations, which result in good agreement with scanning tunnelling spectroscopy experimental data. We also show, by means of simulations performed on a series of trial structures, how changes in the relative orientation of molecules in the unit cell can induce dramatic effects on the electronic band structure and density of states.

2. Structural and computational details

Our simulations were performed within the density functional theory framework, using the generalized gradient approximation (GGA) to the exchange–correlation potential [29]. The all-electron non-relativistic DMol^3 (density functional for theory and molecules [30]) method was used, based on a localized atom-centred numerical polarized basis set employed for the wavefunction expansion, with a finite-size basis cutoff of 9.0 au. Scalar relativistic effects were introduced using a local pseudopotential [31]. As for the Brillouin-zone sampling, we used the Monkhorst–Pack scheme [32] with a $6 \times 6 \times 4$ mesh.

We perform our DFT calculations by introducing as input parameters the structures listed in table 1 for the thin film and bulk polymorphs of pentacene. For the bulk phase we use the experimental lattice parameters with a triclinic Bravais lattice and molecular positions according to Campbell *et al* [11]. Very recently, an experimental work on thin films thermally treated or immersed in organic solvents shows that the bulk phase and the Campbell structure have the same structure (the differences in lattice parameters are less than 1%) [22], as has already been suggested in the literature [33]. Therefore, hereafter we refer to the Campbell structure as the bulk phase. On the other hand, for the thin film we adopt the lattice parameters

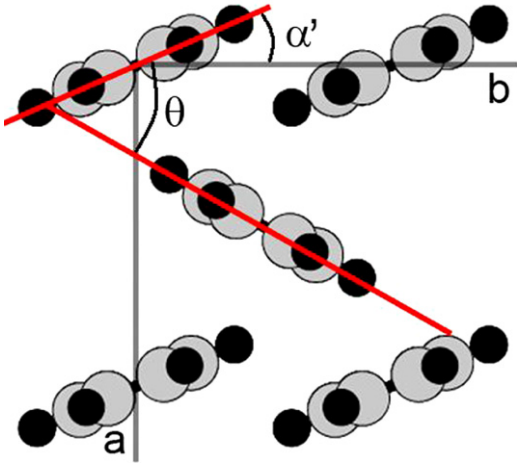

Figure 1. Sketch along the *c* axis of the herringbone crystalline structure of the 'thin film' phase of pentacene. The *a* and *b* directions and the α' and θ angles are shown.

of [25], assuming an orthorhombic configuration with molecules standing perpendicular to the *ab* plane (as suggested by infrared spectroscopy experiments [34]). In figure 1 we show a schematized view of the *ab* plane of the molecular crystalline stacking. The herringbone arrangement is evident. The *a* and *b* directions are sketched, along with the α' and θ angles, which will be useful for the following analyses. α' is the angle formed between the molecular plane of the molecule located at the origin with respect to the *b* direction, whereas θ is the angle between the molecular planes of the two inequivalent molecules in the unit cell. Neither the relative orientation of the molecules nor the orientation of the molecule with respect to the crystalline axes in the thin film phase are known from experiments. Therefore, in the following, we will consider (i) the configuration with $\alpha' = 23°$ and $\theta = 51.9°$, equivalent to the relative orientation in the single-crystal phase and (ii) several different configurations, with various α' and θ angles (see below).

3. Results

We present our results in three distinct subsections, concerning (i) the comparison of DFT calculations of the electronic structure of two distinct polymorphs (thin film and bulk phases, hereafter TF and B), (ii) the comparison with experimental data, and (iii) the effects induced by changes in the tilting of molecules on the electronic structure of the TF polymorph.

3.1. Thin film versus bulk polymorph

In figure 2(a) we report the band structure of the bulk polymorph along the main symmetry directions. The grey zone (yellow in the online edition) indicates the self-consistent energy gap. In the energy range reported, all the orbitals have predominantly a carbon π character. Our results are consistent with a previous work [14] and the small subtle differences can be ascribed to different DFT methodologies and computational details. On the other hand, in figure 2(b) we report the band structure and density of states obtained for the thin film polymorph with $\alpha' = 23°$ and $\theta = 51.9°$, along several symmetry directions. Our results are qualitatively consistent with previous works [23], focused on occupied states. Here, we add the dispersion

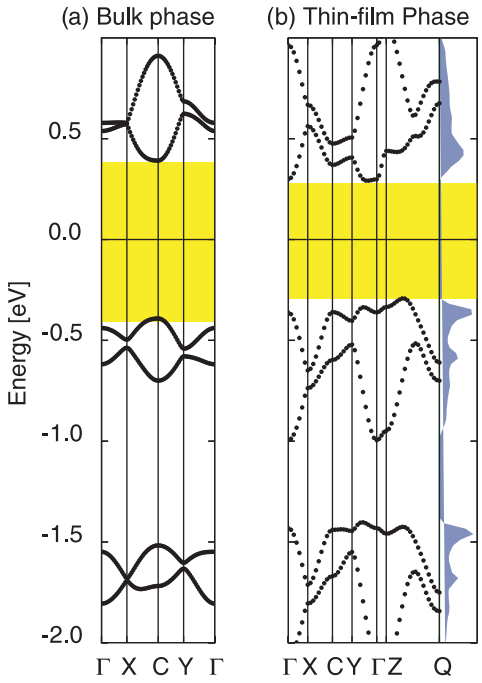

Figure 2. (a) Band structure of the 'bulk' polymorph of pentacene, as reported by Campbell *et al*; (b) band structure (left side) and density of states (right side) of the 'thin film' polymorph of pentacene. Symmetry point labels stand for X $= (0.5, 0, 0)$, Y $= (0, 0.5, 0)$, Z $= (0, 0, 0.5)$, C $= (0.5, 0.5, 0)$ and Q $= (0.5, -1, 0.5)$. Energies are referenced to the Fermi level. Only the HOMO $-$ 1, HOMO and LUMO bands are shown. The DOS has been convoluted with a Gaussian smearing of 0.1 eV.

along other symmetry directions, useful for comparison with other polymorphs and for the global understanding of the electronic structure in the TF phase. We also show the LUMO which, despite the small influence on transport, is extremely important for optical properties. We note from the band structure that the dispersion along the Γ–Z line is rather small, while the band dispersion is much higher in other directions; this confirms that conduction in pentacene occurs in the *ab* plane, which is consistent with previous works [23, 35, 5]. The values for the total HOMO and LUMO bandwidths of the thin film polymorph are respectively 0.69 and 0.77 eV, which are 0.1 eV greater than those reported by de Wijs *et al* [16] for the single-crystal phase, while the energy gap is 0.58 eV, which is 0.1 eV less than the value reported in [16].

In table 2 we report a comparison between the relevant electronic properties of the two polymorphs. First, we observe an increase in the HOMO and LUMO bandwith (BW) and a reduction in the energy band-gap in going from the B to the TF polymorph. For the LUMO the effect is a relative increase of more than 20% of the total bandwidth, while for the HOMO the relative increase is almost 50%. The difference in the energy gap is about 0.2 eV; however, both values are compatible with optical and photoconductive responses of pentacene thin films, as reported by Lee *et al* [36]. Moreover, the directions along which the maximum spread of the HOMO and LUMO bandwidths is observed are interchanged when changing polymorph. In fact, the opening at Γ is larger in TF than the opening in B, while at the C point we observe the opposite behaviour. This can have some consequences for the anisotropy of mobility in the *ab* plane, as has been pointed out previously [16, 23].

Table 2. Energy gap, HOMO and LUMO total bandwidths ($\Delta HOMO_{tot}$ and $\Delta LUMO_{tot}$, respectively) and HOMO and LUMO dispersions at the Γ and C points for the considered bulk and thin film phases. Corrections to the gap values according to 'scissors operators', as defined in [14], are reported in parentheses.

	Thin film	Bulk
Gap (eV)	0.58 (1.88)	0.78 (2.08)
$\Delta HOMO_{tot}$ (eV)	0.69	0.36
$\Delta LUMO_{tot}$ (eV)	0.77	0.57
$\Delta HOMO_{\Gamma}$ (eV)	0.64	0.21
$\Delta LUMO_{\Gamma}$ (eV)	0.67	0.08
$\Delta HOMO_{C}$ (eV)	0.20	0.33
$\Delta LUMO_{C}$ (eV)	0.09	0.55

Table 3. Comparison of HOMO and LUMO bandwidths and energy gaps of the thin film phase of this work with those reported in the literature. Unit cell parameters for [23] are $a = 5.77$ Å, $b = 7.49$ Å, $c = 17.2$ Å, and $\alpha = 73.5°$, $\beta = 75.3°$, $\gamma = 91.2°$; unit cell parameters for [24] are $a = 7.50$ Å, $b = 5.92$ Å, and $c = 15.35$ Å, and $\alpha = \beta = 90°$, $\gamma = 91°$.

	This work	Reference [23]	Reference [24]
HOMO bandwidth	0.69	0.3	0.56
LUMO bandwidth	0.77	—	0.33
HOMO–LUMO gap	0.58	—	0.44

Let us briefly comment on the comparison with previous theoretical works focused on the thin film phase. In table 3 we report the HOMO and LUMO bandwidths and the energy gap values for the thin film polymorph as reported in [23, 24]. With respect to reference [23], we recall that in such work only the HOMO state is reported along three symmetry directions for the thin film polymorph. The overall HOMO bandwidth is almost 0.4 eV lower than that of our calculation. Moreover, in [23] the authors claim that the bandwidth of the TF phase is four times larger than the BW in other polymorphs. Indeed, this is true along the Γ–X and Γ–Y direction, but is no longer valid when considering other symmetry directions. For example, in the Campbell structure (see figure 2(a)), the dispersion is a maximum at the C point (i.e. the midpoint of the edge in the *a*–*b* in-plane Brillouin zone), which was not explicitly reported in [23]. Therefore, if we consider the dispersion in the whole Brillouin zone, we note that the BW is larger than in the B phase, but not by as much as four times, outlining the importance of sampling over different symmetry lines to give a thorough description of the electronic structure. Finally, we remark that the band structure for our thin film polymorph is in qualitative agreement with the results of [24]. However, we find some differences when considering the HOMO and LUMO bandwidth and the energy gap values. In fact, when compared with reference [24], our results show a larger value for the HOMO (0.13 eV) and LUMO (0.44 eV) bandwidths, along with a smaller value for the energy gap (0.14 eV). Such differences can be ascribed to computational parameters, to the fact that the unit cell is not exactly the same as ours, and, most importantly, to the relative molecular orientation (not specifically reported in [24]) which may be different from the one considered in the present work.

3.2. Thin film: theory versus experiment

The electronic band calculations performed on the thin film phase polymorph can be compared with experimental scanning tunnelling spectroscopy (STS) measurements previously

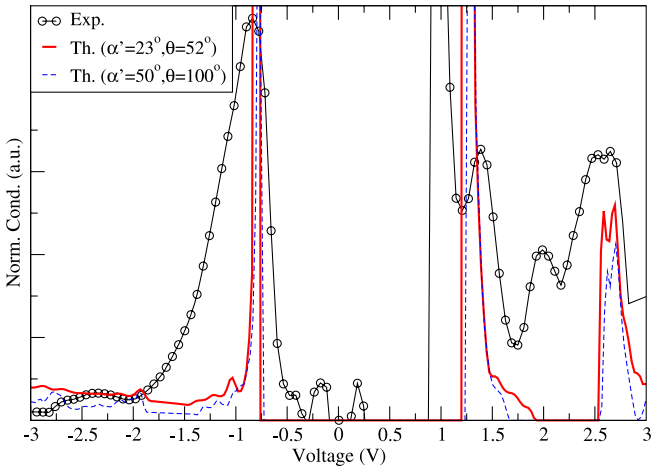

Figure 3. Comparison between the experimental (circles) and theoretical (bold (red) continuous line $\alpha' = 23°$ and $\theta = 52°$; blue dashed line $\alpha' = 50°$ and $\theta = 100°$) normalized conductances. The experimental details are reported elsewhere [28].

performed by some of us on a 5 nm film of pentacene in the thin film phase and described in detail elsewhere [28]. Recall that STS is a technique that allows us to study, with subnanometric spatial resolution, the electronic structure around the Fermi level in the range of a few eVs, both for the empty states as well as for the filled states of metals and semiconductors with an energy resolution $\leqslant 4$ kT. In fact, it is well known that the tunnelling current, or better the normalized conductance $(\mathrm{d}I/\mathrm{d}V)/(I/V)$, is proportional to the density of states [37]. Starting from the theoretical density of states of the thin film polymorph (see figure 2), we calculate the $I(V)$ curve and the normalized conductance, according to equations (1) and (2):

$$I(V) = \int_{-\infty}^{+\infty} \rho_{\mathrm{s}}(E - eV)\rho_{\mathrm{t}}(E)T(E, eV) \times [f(E - eV) - f(E)]\,\mathrm{d}E, \quad (1)$$

where

$$T(E, eV) = \exp\left(-2z\sqrt{\frac{2m}{\hbar^2}\left(\Phi - E + \frac{eV}{2}\right)}\right) \quad (2)$$

is the tunnelling exponential factor from the WKB (Wentzel–Kramers–Brillouin) approximation (assuming a workfunction Φ of 4 eV and a tip–sample distance z of 5 Å), $f(E)$ is the Fermi–Dirac distribution function; a constant tip density of states $\rho_{\mathrm{t}}(E)$ has been chosen [38]. In figure 3 we report the comparison between experimental (circles) and theoretical (bold (red) continuous line) curves. Due to the well-known underestimate of the band-gap within DFT, we performed a rigid shift of the unoccupied levels so as to enlarge the underestimated gap; the magnitude of the shift was chosen to be 1.3 eV, according (within 0.1 eV) to the results of accurate calculations performed within the so-called 'GW'-approach on several pentacene polymorphs [14]. Once the Fermi level is manually shifted to make the position of the theoretical HOMO and of the experimental data coincide, there is a good agreement between theoretical curves and the STS measurements, not only for the energy position of the HOMO and of the LUMO, but also for the HOMO $-$ 1 and LUMO $+$ 1 levels. Therefore, we infer that our DFT description of the pentacene TF phase is, to a large extent, reliable. Moreover, since the geometry is an important factor in determining the overall electronic structure—as clearly

shown below—we suggest that the molecular stacking presently considered can be a possible candidate for the relative orientation in the TF phase.

3.3. Thin film: trial structures

In order to rationalize our results, we perform DFT simulations on an extensive series of trial structrures, where the values of α' and θ are changed.

It is well known that DFT lacks accuracy when describing weakly bonded systems. In this case, van der Waals interactions between molecules are expected to occur, and it is therefore hard to estimate quantitatively which is the most stable structure, according to a pure DFT approach and within the limits of our computational parameters (such as exchange–correlation potential, forces minimization, **k**-point sampling, etc). However, we give some qualitative hints based on the DFT total energies. In particular, we find that the previously considered structure (i.e. $\alpha' = 23°$ and $\theta = 51.9°$) is indeed the most stable (by as much as a few tenths of eV per molecule) with respect to other systems, suggesting the possibility that this is indeed a good candidate for the experimentally realized crystalline arrangement. However, we stress that our main aim here is not to focus on the stability of the different systems, but rather to examine the changes induced by the molecular relative orientation on the relevant electronic properties: all those structures in which the tilt angles have been significantly varied (some of them reaching an unrealistic molecular stacking) have the sole aim of underlining the dramatic changes induced by the molecular orientation inside the unit cell.

In figures 4(a)–(h) we report a summary of the density of states calculated for different structures. In panel (a) we report the results for a structure with just one molecule in the unit cell; in this case, the DOS reflects the undispersed molecular levels. Incidentally, we point out that our simulations for the pentacene molecule are in excellent agreement with recent results of Endres *et al* [19], in particular as far as the symmetries and the orbital character of HOMO and LUMO are concerned. In the trial structure shown in panel (b) we insert two molecules in the unit cell parallel to the a axis. In this case we recover a graphite-like structure with an almost zero gap: therefore, the clear semiconducting behaviour—experimentally observed and theoretically confirmed in several structures (see, for example, figure 2(b))—is a consequence of the relative tilting of the molecules. The importance of the molecular arrangement in the unit cell is evident in the extreme case reported in panel (f): this non-realistic structure is meant to show that the close distance between molecules in $(1/2, 1/2, 0)$ in adjacent unit cells can even result in metallic behaviour. A similar situation can be observed in panel (h), where the closing of the gap is due to the almost parallel arrangement of the molecules. On the other hand, as shown in panels (c), (e) and (g), if we put the molecules in the opposite situation (i.e. perpendicular to each other), we observe the induced opening of the gap. Let us further compare the DOS for these panels with the more realistic structure for the thin film phase, panel (d): the major difference concerns the LUMO bandwidth, which seems to be larger than in the (c), (e) and (g) cases. In table 4 we show a summary of the HOMO and LUMO bandwidths, as well as of the energy gap for all the configurations considered. First of all, as expected, the opening of the gap is inversely proportional to the HOMO and LUMO bandwidth enlargements, which, as for other electronic properties, strongly depend on the θ angle. This is indeed evident from the comparison between figures 4(e) and (g), both having $\alpha' = 45°$ but differing for the values of θ: the bandwidths of the HOMO and, even more markedly, of the LUMO are strongly different. However, the α' angle is also important, as is shown by the comparison between figures 4(f) and (d), having the same $\theta = 52°$ but differing in the value of α'. Again, the two electronic structures are remarkably different, outlining once more the strong dependence of the electronic structure on the orientational details of the herringbone arrangement.

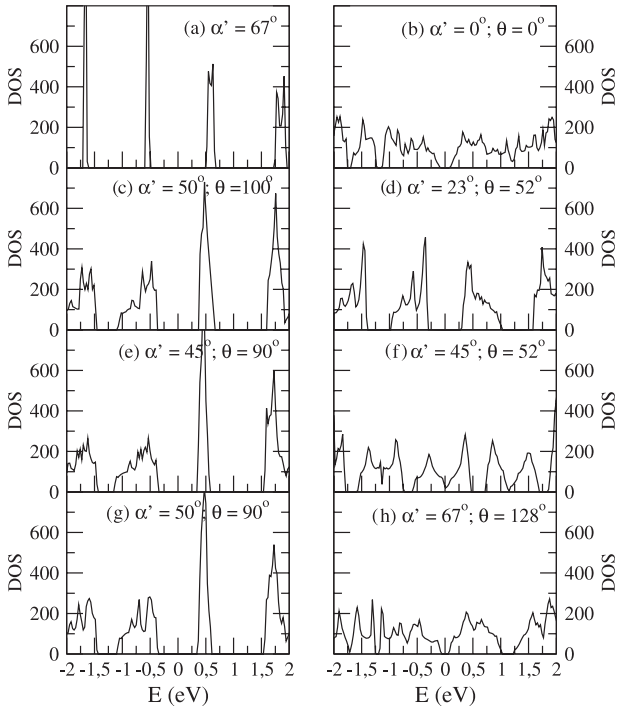

Figure 4. Density of states of the trial structures for the following configurations: (a) one molecule per unit cell, $\alpha' = 67°$; two molecules per unit cell with (b) $\alpha' = 0°$ and $\theta = 0°$; (c) $\alpha' = 50°$ and $\theta = 100°$; (d) $\alpha' = 23°$ and $\theta = 52°$; (e) $\alpha' = 45°$ and $\theta = 90°$; (f) $\alpha' = 45°$ and $\theta = 52°$; (g) $\alpha' = 50°$ and $\theta = 90°$; (h) $\alpha' = 67°$ and $\theta = 128°$.

Table 4. Summary of relevant electronic properties (such as the bandwidths $\Delta\text{HOMO}_{\text{tot}}$ and $\Delta\text{LUMO}_{\text{tot}}$ and the energy band-gap) in the different thin film phases as a function of the α' and θ values. All values are in eV.

α' (deg)	θ (deg)	$\Delta\text{HOMO}_{\text{tot}}$ (eV)	$\Delta\text{LUMO}_{\text{tot}}$ (eV)	Gap (eV)
0	0	1.06	1.15	0.14
50	100	0.73	0.3	0.73
23	52	0.69	0.77	0.58
45	90	0.83	0.25	0.69
50	90	0.77	0.28	0.67
67	128	1.15	0.99	0.11

Let us finally comment on the comparison with experimental spectra, discussed in the previous section. When performing the comparison between STS and other structures with different θ and α' angles, we are able to exclude several different molecular arrangements (such as those leading to the electronic structure shown in figures 4(b), (f) and (h). On the other hand, when performing the comparison between STS and system (c)—taken as being representative for the system with a large HOMO BW but relatively small LUMO BW—the comparison (figure 3 dashed line) is quite satisfactory. In particular, it is only slightly worse than in case (d) as far as the LUMO BW is concerned, but the other peak positions and energy spreading are in good agreement with experiments as well. Therefore, we cannot

exclude the real molecular stacking of having an arrangement with molecular planes closer to a 'perpendicular-like' situation (i.e. $\theta \sim 90°$) rather than a more tilted system (i.e. $\theta = 52°$).

4. Conclusions

First-principles simulations have been performed for a pentacene organic crystal in the 'thin film' phase, focusing on the effect of the relative molecular orientation on the electronic structure. Indeed, we find a crucial dependence of the HOMO and LUMO bandwidths as well as of the band-gap on both the angles that determine the molecular stacking. In particular, assuming a relative molecular orientation similar to the single-crystal phase, both the HOMO and LUMO bandwidths increase by a few tenths of an electron volt with respect to the bulk phase, with a consequent reduction in the energy band-gap. By means of a comparison with scanning tunnelling spectroscopy measurements performed on pentacene thin films, we find the HOMO $-$ 1, HOMO, LUMO and LUMO $+$ 1 orbitals to be well reproduced by our *ab initio* simulations, both in energy position (provided a rigid opening of the gap, due to the well-known DFT errors in describing excited states) and bandwidth. Our results suggest the assumed molecular arrangement as a possible candidate for the orientation in real pentacene 'thin film' samples, and call for further experimental work aimed at determining the real mutual molecular orientation.

References

[1] Reese C, Roberts M, Ling M and Bao Z 2004 *Mater. Today* **7** 20
[2] Mattheus C C, Dros A B, Baas J, Oostergetel G T, Meetsma A, de Boer J L and Palstra T T M 2003 *Synth. Met.* **138** 475
[3] Dimitrakopoulos C D and Malenfant P R L 2002 *Adv. Mater.* **14** 99
[4] Mayer A C, Ruiz R, Headrick R L, Kazimirov A and Malliaras G G 2004 *Org. Electron.* **5** 257
[5] Jurchescu O D, Baas J and Palstra T T M 2004 *Appl. Phys. Lett.* **84** 3061
[6] Lin Y Y, Gundlach D J, Jackson T N and Nelson S F 1997 *IEEE Trans. Electron Devices* **44** 1325
[7] Wang L, Fine D, Jung T, Basu D, von Seggern H and Dodabalapur A 2004 *Appl. Phys. Lett.* **85** 1772
[8] Daraktchiev M, von Mhlenen A, Nesch F, Schaer M, Brinkmann M, Bussac M N and Zuppiroli L 2005 *New J. Phys.* **7** 133
[9] Kim S S, Choi Y S, Kim K, Kim J H and Im S 2003 *Appl. Phys. Lett.* **82** 639
[10] Voz C, Puigdollers J, Martýn I, Munoz D, Orpella A, Vetter M and Alcubilla R 2005 *Sol. Energy Mater. Sol. Cells* **87** 567
[11] Campbell R B, Monteath Robertson J and Trotter J 1962 *Acta Crystallogr.* **15** 289
[12] Mattheus C C, de Wijs G A, de Groot R A and Palstra T T M 2003 *J. Am. Chem. Soc.* **125** 6323
[13] Della Valle R G, Brillante A, Venuti E, Farina L, Girlando A and Masino M 2004 *Org. Electron.* **5** 1
[14] Tiago M L, Northrup J E and Louie S 2003 *Phys. Rev.* B **67** 115212
[15] Cheng Y C, Silbey R J, da Silva Filho D A, Calbert J P, Cornil J and Bredas J L 2003 *J. Chem. Phys.* **118** 3764
[16] de Wijs G A, Mattheus C C, de Groot R A and Palstra T T M 2003 *Synth. Met.* **139** 109
[17] Deng W Q and Goddard W A III 2004 *J. Phys. Chem.* B **108** 8614
[18] Haddon R C, Chi X, Itkis M E, Anthony J E, Eaton D L, Siegrist T, Mattheus C C and Palstra T T M 2002 *J. Phys. Chem.* B **106** 8288
[19] Endres R G, Fong C Y, Yang L H, Witte G and Woll Ch 2004 *Comput. Mater. Sci.* **29** 362
[20] Hummer K and Ambrosch-Draxl C 2005 *Phys. Rev.* B **72** 205205
[21] Siegrist T, Kloc C, Schon J H, Batlogg B, Haddon R C, Berk S and Thomas G A 2001 *Angew. Chem. Int. Edn Engl.* **40** 1732
[22] Yoshida H and Sato N 2006 *Appl. Phys. Lett.* **89** 101919
[23] Troisi A and Orlandi G 2005 *J. Phys. Chem.* B **109** 1849
[24] Doi K, Yoshida K and Nakano H 2005 *J. Appl. Phys.* **98** 113709
[25] Ruiz R, Mayer A C, Malliaras G G, Nickel B, Scoles G, Kazimirov A, Kim H, Headrick R L and Islam Z 2004 *Appl. Phys. Lett.* **85** 4926
[26] Fritz S E, Martin S M, Frisbie C D, Ward M D and Toney M F 2004 *J. Am. Chem. Soc.* **126** 4084

[27] Mayer A C, Kazimirov A and Malliaras G G 2006 *Phys. Rev. Lett.* **97** 105503
[28] Parisse P, Passacantando M and Ottaviano L 2006 *Appl. Surf. Sci.* **252** 7469
[29] Perdew J P, Burke K and Ernzerhof M 1996 *Phys. Rev. Lett.* **77** 3865
[30] Delley B 1990 *J. Chem. Phys.* **92** 508
Delley B 2000 *J. Chem. Phys.* **113** 7756
[31] Delley B 1998 *Int. J. Quantum Chem.* **69** 423
[32] Monkhorst H J and Pack J D 1976 *Phys. Rev.* B **13** 5188
[33] Farina L, Brillante A, Della Valle R G, Venuti E, Amboage M and Syassen K 2003 *Chem. Phys. Lett.* **375** 490
[34] Hosoi Y, Okamura K, Kimura Y, Ishii H and Niwano M 2005 *Appl. Surf. Sci.* **244** 607
[35] Parisse P, Passacantando M, Picozzi S and Ottaviano L 2006 *Org. Electron.* **7** 403
[36] Lee J, Kim S S, Kim K, Kim J H and Im S 2004 *Appl. Phys. Lett.* **84** 1701
[37] Märtensson P and Feenstra R M 1989 *Phys. Rev.* B **39** 7744 and references therein
[38] Ressel B, Di Teodoro C, Profeta G, Ottaviano L, Chab V and Prince K C 2004 *Surf. Sci.* **128** 562